

Short Communication

Incorporating Oxygen CoP Nanosheets: Facile Synthesis and Application for Supercapacitor Electrodes

Jia Wang, Xuan Ren, Liang Chen, and Baocheng Wang*

Taiyuan University of Technology, Taiyuan, Shanxi, P.R.China

*E-mail: tylgdwangjia@sina.com

Received: 4 August 2018 / Accepted: 16 September 2018 / Published: 1 October 2018

As an effective way, surface functionalization can modulate the electrochemical properties of nanomaterials for supercapacitors. The Co_3O_4 nanosheets as the precursor have been synthesized using a solvothermal reaction followed by a high-temperature calcination reaction. Oxygen-incorporating CoP nanosheets were obtained via a high-temperature phosphating reaction. The obtained samples have been characterized by X-ray diffraction and transmission electron microscopy. The electrochemical results displayed that the oxygen-incorporating CoP nanosheets are promising anode material for high-performance supercapacitor devices. The specific capacitance of the sample could be calculated to 416, 345 and 317 F g^{-1} at a current density of 2, 5 and 10 A g^{-1} , respectively. Even after 900 cycles, the capacitive retention of the oxygen-incorporating CoP nanosheets electrode was 97% and it remained unchanged, manifesting that such a supercapacitor displays a good electrochemical cycling stability. The high specific capacity, long cycle stabilities as well as great rate capability make the oxygen-incorporating CoP nanosheets a good candidate for high-performance supercapacitors.

Keywords: CoP nanosheets, Oxygen incorporation, Supercapacitors, Polymers, Electronic materials

1. INTRODUCTION

Over the past decades, the energy crisis due to the environmental pollution and global warming hugely stimulate world-wide research interest in environment-friendly and renewable power resources and valid energy storage systems [1-3]. In particular, supercapacitors as one of the most significant candidates for new generation energy storage systems stands out, due to their large power densities, long stable cyclic property, low maintenance and environmental benign. As is known to all, supercapacitors can be generally divided into two categories, the first one is electric double-layer capacitors (EDLCs) based on the electrostatic model and no redox reaction is involved, the second one is pseudo-capacitors based on the fast surface redox reaction under certain potentials [4, 5]. It is worth noted that the specific capacitances delivered by pseudo-capacitors are much larger than that of

EDLCs due to reversible multiple redox reaction occurred both at the surface and near-surface of the electrode. Thus, tremendous endeavors have been devoted to explore proper pseudocapacitive electrode materials around the world.

Low cost transition metal oxides and hydroxides have been widely investigated as feasible redox-active materials for pseudo-capacitors, such as MnO_2 [6], Ni(OH)_2 [7], Co(OH)_2 [8], CoO_x [9] etc. Among these materials, cobalt oxide materials are emerging as one of the favorable candidates for pseudo-capacitors due to their low cost, high theoretical capacitance, and great reversibility. However, the capacitances of most reported CoO_x materials are still far behind their theoretical capacitances, which is due to their immense inferior electrical conductivity. To improve the performance of CoO_x materials, highly conductive materials were used to fabricate nanostructured composites with CoO_x [10]. However, the limited surface chemical reactivity of nanostructured CoO_x electrode still hindered their practical applications. In recent years, owing to higher electronic conductivity, transitional-metal phosphides, as a new sort of multifunctional materials, have been widely emerged with remarkable electrochemical activities for Li/Na batteries[11], electrocatalysis[12], and advanced electrochemical supercapacitors[13, 14].

Herein, it is reported there is a new strategy to modify the surface of CoP nanosheets by oxygen incorporation. According to recent works by Xu and coworkers[15], it is found that oxygen incorporation into Co₂P could surprisingly enhance the hydrogen evolution reaction catalytic activity in alkaline solution due to the synergistic regulation of water dissociation and optimization of hydrogen adsorption free energy. Enlightened by this study, we predicted that functionalizing the surface of CoP nanosheet with oxygen could motivate high chemical reactivity for high-speed and efficient faradaic reactions. In current work, a strategy to fabrication oxygen-incorporating CoP nanosheets was developed and enhanced specific capacitance was found substantially compared with the prepared Co_3O_4 nanosheets.

2. MATERIALS AND METHODS

2.1 Synthesis of Co_3O_4 nanosheets

0.2 g P123 was added into the mixed solution with 13 mL ethanol and 1 mL water to form a clear solution with 15 minutes' stirring. Then 0.125 g cobalt acetate and 0.07 g hexamethylenetetramine were dissolved in the solution. After stirring for another 15 min, 13 mL of ethylene glycol was added into the solution. The above solution was aged for one day after stirring for 30 min. The solution was then transferred into a Teflon autoclave and heated at 170 °C for 2 h. The products of the solvothermal reaction were gathered and washed with deionized water and absolute ethanol completely. After dried at 50 °C overnight in a vacuum oven, the sample was calcined for 2 h at 350 °C in air with a heating rate of 1 °C min⁻¹ in order to produce crystallized Co_3O_4 nanosheets[16].

2.2 Synthesis of oxygen-incorporating CoP nanosheets

To prepare oxygen-incorporating CoP nanosheets, Co_3O_4 nanosheets and NaH_2PO_2 were put at

their respective positions in a porcelain boat with the latter one at upstream side of the furnace. The weight ratio for Co_3O_4 nanosheets and NaH_2PO_2 was 1:10. After flushed with Ar, the center of the furnace was enhanced to $350\text{ }^\circ\text{C}$ at a ramp rate of $1\text{ }^\circ\text{C min}^{-1}$ and held for 2 h, and then naturally cooled to surrounding temperature under argon atmosphere.

2.3 Structure characterization

X-ray powder diffraction (XRD) patterns were achieved on a Bruker D8 advanced X-ray diffractometer with Cu K α radiation (1.5418 \AA). The structure and morphology of the products were observed by a field emission scanning electron microscope (SEM, SUPRATM 55), a transmission electron microscope (TEM, JEM-1011) with an accelerating voltage of 100 kV.

2.4 Electrochemical measurements

The working electrodes were typically composed of 80% of obtained samples (Co_3O_4 nanosheets or CoP nanosheets), 10% of acetylene black as conducting binder, and 10% of polyvinylidene difluoride as mechanical binder. The mixture is then pressed onto a nickel foam ($1\text{ cm} \times 2.0\text{ cm}$) at a pressure of 5 MPa and dried under vacuum at 50°C for 24h. Electrochemical measurements on the capacitive performance were conducted with a CHI 660E electrochemical workstation (Shanghai, China) in an aqueous KOH electrolyte (6.0 M) using a three-electrode configuration, where a platinum plate serves as the counter electrode and a HgO/Hg as the reference electrode. The gravimetric specific capacitance of the electrodes was calculated from the CP profiles based on the the following equation:

$$\text{SC} = It/\Delta V \quad (1)$$

where I , t , and ΔV denote the discharging current (A g^{-1}), the discharging time (s), and the discharging potential range (V), respectively.

3. RESULTS AND DISCUSSION

Figure 1a manifests the XRD pattern of the Co_3O_4 nanosheets. All the diffraction peaks are in line with the cubic Co_3O_4 (JCPDS No. 43-1003, space group Fd3m). We performed transmission electron microscopy (TEM) analyses on Co_3O_4 nanosheets. These nanosheets can be obviously distinguished in the low-magnification TEM images (Figure 1b-d). They present in the form of groups of nanosheets, which assembled as flower-like structures. The edges of the nanosheets rolled up owing to surface tension which has a similarity to the general behavior of graphene, indicating the thickness of the nanosheets is very low.

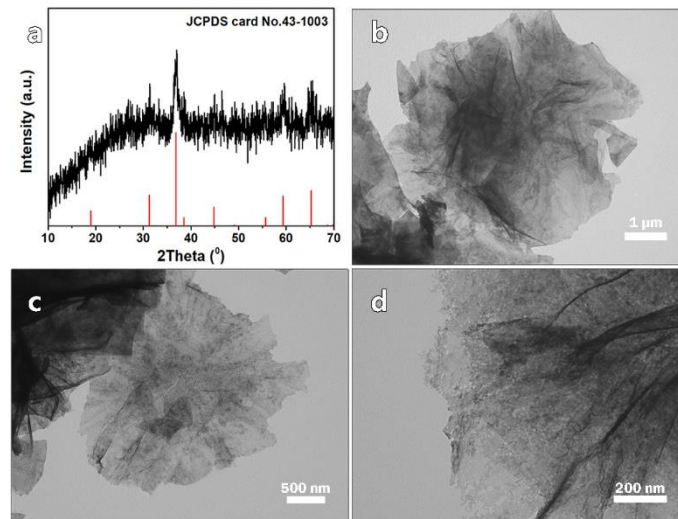


Figure 1. The XRD pattern (a) and TEM images (b-d) of Co₃O₄ nanosheets.

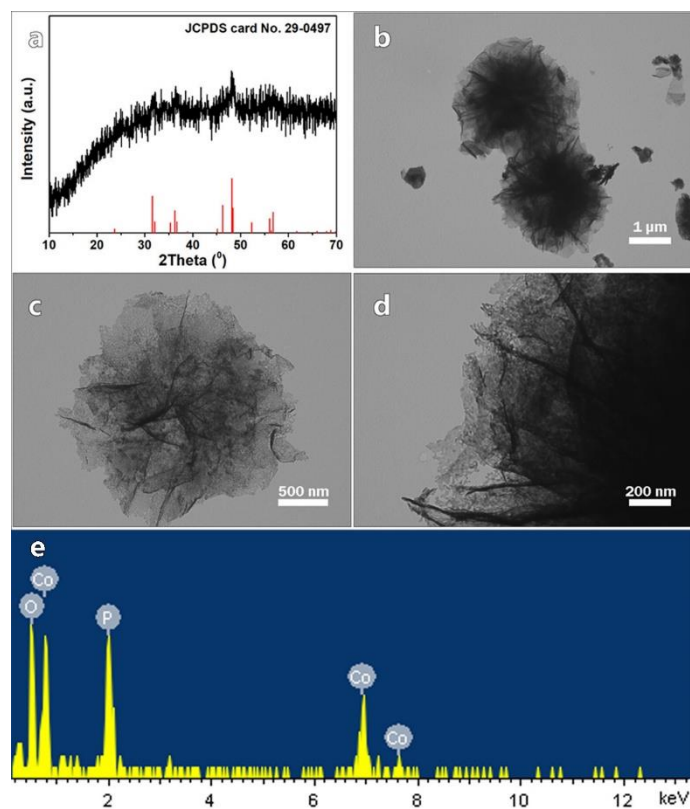


Figure 2. The XRD pattern (a) , TEM images (b-d) ,and EDS results (e) of oxygen-incorporating CoP nanosheets.

The oxygen-incorporating CoP nanosheets samples were fabricated by a simple phosphating reaction by further annealing the as-prepared Co₃O₄ nanosheets in Ar atmosphere in the presence of NaH₂PO₂ at a controlled reaction temperature. The decomposition of NaH₂PO₂ can generate PH₃, which further reduces Co₃O₄ nanosheets to CoP. Appropriate reaction conditions would lead to

oxygen-incorporating in CoP nanosheets on account of the existence of oxygen atoms in the Co_3O_4 nanosheets. The phosphate ion functionalized Co_3O_4 nanosheets could be obtained at a temperature of 250°C [17]. The phosphating extent of cobalt precursor increased as the temperature increased. The oxygen-incorporating CoP nanosheets could be obtained at a temperature of 350°C . The XRD pattern (Figure 2a) of the phosphide product is consistent with CoP standard pattern (JCPDS No. 29-0497, space group Pnma). TEM image (Figure 2b-d) demonstrates that the product still preserves its flower-like morphology, but with rough surface. The energy-dispersive X-ray spectrometry (EDS) of the product in selected area is shown in Figure 2e the EDS results revealed the presence of Co, P, O elemental peaks, indicating oxygen functionalization on the surface of CoP nanosheets.

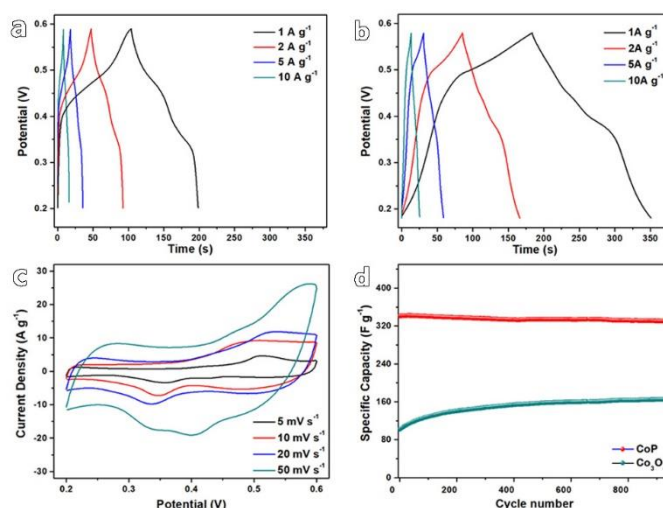


Figure 3. The galvanostatic charge-discharge curves at various current densities of Co_3O_4 nanosheets (a); oxygen-incorporating CoP nanosheets (b); Cyclic voltammograms of oxygen-incorporating CoP nanosheets at varying sweep rates (c); Cycle performance of oxygen-incorporating CoP nanosheets at a current density of 5 A g^{-1} (d).

With potential window between 0.2 and 0.6 V (vs. HgO / Hg), the galvanostatic charge-discharge measurements were conducted to investigate the specific capacitances of the electrodes. The nonlinear curves of Co_3O_4 nanosheets and oxygen-incorporating CoP nanosheets shown in Figure 3a-b confirm their faradaic capacitance behavior. The legible charge-discharge plateau is primarily due to the reversible redox reactions in a certain potential range at the surface and the interior of the electrodes, as well as the charge accumulation at the electrode/electrolyte interface. At the equal current density, the oxygen-incorporating CoP electrode appears a much longer discharging time than the Co_3O_4 , indicating that the oxygen-incorporating CoP electrode presents higher specific capacitance values. Based on the curves of both electrodes, the calculated specific capacitance at 1 A g^{-1} are 251, 439 F g^{-1} for Co_3O_4 nanosheets and oxygen-incorporating CoP nanosheets, respectively. The capacitance of oxygen-incorporating CoP nanosheets is almost twice as large as that of Co_3O_4 nanosheets. The existence of oxygen atoms could regulate the dissociation of water, resulting the increasing of the number of active surface site[15]. It can also help improve the capacitance of material,

and at the same time, reduce the electron transfer resistance of the material[13]. The specific capacitance of oxygen-incorporating CoP nanosheets could be calculated to 416, 345 and 317 F g⁻¹ at a current density of 2, 5 and 10 A g⁻¹, respectively. The capacitances slightly diminish with the increase of the current densities, which indicates that the redox reaction is allowed to occur rapidly in these materials at high galvanostatic current densities.

Figure 3c shows the cyclic voltammetry (CV) curves of oxygen-incorporating CoP nanosheets at different scan rates of 5, 10, 20, and 50 mV s⁻¹. A couple of distinct redox peaks of CV curves is derived from reversible faradaic reactions, obviously displaying the conventional faradaic behaviors of this battery-type electrode. With the increasing of scan rate, the potential of the oxidation peak increases gradually, and the potential of reduction shifts to the low potential. As the scanning rate increases, the peak current also presents an increasing trend. It can be also seen that the shapes of these CV curves can be maintained, revealing that the fast-redox reactions take place in the electrode.

Figure 3d reveals the cycling performance of the Co₃O₄ nanosheets and oxygen-incorporating CoP nanosheets electrodes at a current density for 5 A g⁻¹. Particularly, the specific capacitance of the Co₃O₄ nanosheets electrode increases gradually during the preceding cycles, which is mainly attributed to an incipient activation process in the electrode. Furthermore, after 900 cycles, the capacitive retention of the oxygen-incorporating CoP nanosheets electrode was 97% and it remained unchanged, indicating that such a supercapacitor takes on a great electrochemical cycling stability.

Compared with other similar electrode materials for supercapacitors, the oxygen-incorporating CoP nanosheets display better performance. The specific capacitance of MnO₂ is 325 F g⁻¹ at a current density of 1 A g⁻¹, and the capacitive retention is 90% after 5000 cycles[6]. The specific capacitance of Ni(OH)₂ is 235 F g⁻¹ at a current density of 1 A g⁻¹, and the capacitive retention is 83% after 1000 cycles[7].

4. CONCLUSIONS

In conclusion, the oxygen-incorporating CoP nanosheets were synthesized via a solvothermal method, followed by a two-step high temperature treatment. The structure of the prepared product was characterized by XRD and TEM. The resulted electrochemical properties exhibited that the obtained product is a promising electrode material for high-performance supercapacitor devices.

ACKNOWLEDGEMENTS

This study was support by the National Natural Science Foundation of China (Grant No. 21706171).

References

- 1 X. Lei, K. Yu, R. J. Qi and Z. Q. Zhu, *Chem. Eng. J.*, 347(2018)607-617.
- 2 J. L. Xie, Z. Y. Zhan, S. W. Zhang, G. Li, H. C. Xia, Y. F. Yang and J. Xiong, *Mater. Lett.*, 226(2018)30-33.
- 3 Y. H. Jin, C. C. Zhao, Q. L. Jiang and C. W. Ji, *Appl. Surf. Sci.*, 450(2018)170-179.

- 4 V. Augustyn, P. Simon and B. Dunn, *Energy Environ. Sci.*, 7(2014)1597-1614.
- 5 J. F. Sun, C. Wu, X. F. Sun, H. Hu, C. Y. Zhi, L. R. Hou and C. Z. Yuan, *J. Mater. Chem. A*, 5(2017)9443-9464.
- 6 M. Huang, F. Li, F. Dong, Y. X. Zhang and L. L. Zhang, *J. Mater. Chem. A*, 3(2015)21380-21423.
- 7 L. S. Zhang, Q. W. Ding, Y. P. Huang, H. H. Gu, Y. E. Miao and T. X. Liu, *ACS Appl. Mater. Interfaces*, 7(2015)22669-22677.
- 8 L. Wang, C. Lin, F. X. Zhang and J. Jin, *ACS Nano*, 8(2014)3724-3734.
- 9 C. Feng, J. F. Zhang, Y. He, C. Zhong, W. B. Hu, L. Liu and Y. D. Deng, *ACS Nano*, 9(2015)1730-1739.
- 10 C. Z. Yuan, L. Yang, L. R. Hou, J. Y. Li, Y. X. Sun, X. G. Zhang, L. F. Shen, X. J. Lu, S. L. Xiong and X. W. Lou, *Adv. Funct. Mater.*, 22(2012)2560-2566.
- 11 G. H. Li, H. Yang, F. C. Li, J. Du, W. Shi and P. Cheng, *J. Mater. Chem. A*, 4(2016)9593-9599.
- 12 J. Q. Tian, Q. Liu, A. M. Asiri and X. P. Sun, *J. Am. Chem. Soc.*, 136(2014)7587-7590.
- 13 Y. Lan, H. Zhao, Y. Zong, X. Li, Y. Sun, J. Feng, Y. Wang, X. Zheng and Y. Du, (2018)
- 14 X. Li, H. J. Wu, A. M. Elshahawy, L. Wang, S. J. Pennycook, C. Guan and J. Wang, *Adv. Funct. Mater.*, 28(2018)10.
- 15 K. Xu, H. Ding, M. X. Zhang, M. Chen, Z. Hao, L. Zhang, C. Z. Wu and Y. Xie, *Adv. Mater.*, 29(2017)6.
- 16 Z. Q. Sun, T. Liao, Y. H. Dou, S. M. Hwang, M. S. Park, L. Jiang, J. H. Kim and S. X. Dou, *Nat. Commun.*, 5(2014)9.
- 17 T. Zhai, L. M. Wan, S. Sun, Q. Chen, J. Sun, Q. Y. Xia and H. Xia, *Adv. Mater.*, 29(2017)8.